

Spatial and Temporal Variations of Climate in Europe

Vladimir Kossobokov^{1,2}, Jean-Louis Le Mouél², Claude Allègre²

¹Institute of Earthquake Prediction Theory and Mathematical Geophysics, Russian Academy of Sciences, Moscow, Russia

²Institut de Physique du Globe de Paris, Paris, France

Email: volodya@mitp.ru

Received July 4, 2012; revised August 7, 2012; accepted August 16, 2012

ABSTRACT

Temperature series of the original individual measurements of the minimum and maximum daily temperatures from 24 stations located in different regions of Europe are considered with the objective of studying the stability or the variability of the “climate” in time and space. The patterns of the temperature statistics, the shapes of probability density functions, in particular, at different places and times allow comparisons based on the Kolmogorov-Smirnov test, the Shannon entropy, and cluster analysis, used separately or in combination for the purposes of quantitative climate classification.

Keywords: Daily Air Temperature; Climate; Classification; Empirical Distribution Function; Entropy; Cluster Analysis

1. Introduction

In two recent papers, we analyzed the longest temperature series in Europe (*i.e.*, Prague, Bologna, and Uccle) available from the European Climate Assessment and Dataset [1]. The two former papers focused on the investigation of a solar effect on temperature series [2,3]. In the present paper we consider the temperature series from 24 stations located in different regions of Europe with the objective of studying the stability or the variability of the “climate” in time and space. For that, instead of considering series of temporal averages like, e.g., the series of monthly temperatures of the Northern Hemisphere, or of Central England, etc., we make use in full of the original individual measurements of the minimum and maximum daily temperatures and compare statistics of their distributions at different places and times.

2. The Data

We use the data set of the daily air temperature observations over more than a hundred years (in one case, more than two hundred years) published in 2007 by the European Climate Assessment and Data Set, ECA&D. More precisely, we have extracted from ECA&D the long series of minimum and maximum temperatures ($TN = T_{\min}$ and $TX = T_{\max}$, respectively) at stations that sample different climatic regions of Europe. We did not retain the very long series of Central England [4] since we chose using non-blended data. The list of the selected 24 stations (ordered from W to E), with their coordinates (latitude and longitude) and length of temperature series, are given in **Table 1**; their geographical distribution, along

with climate classification, is shown in **Figure 1**.

We essentially compute and plot the empirical probability functions (*pf*s), $F_i(\tau)$, and probability density (distribution) functions (*pdf*s), $f_i(\tau)$, of the different series T over different time intervals $Y_i = (y_{i+1}, y_i)$, where $y_i - y_{i+1} = \Delta y$ years. By definition, for a given time interval, $F_i(\tau)$ and $f_i(\tau)$ are the ratios of the number of values from the temperature intervals $T \leq \tau$ and $T \leq \tau < \tau + \Delta\tau$ to the total number of values T , respectively. Of course *pf*s and

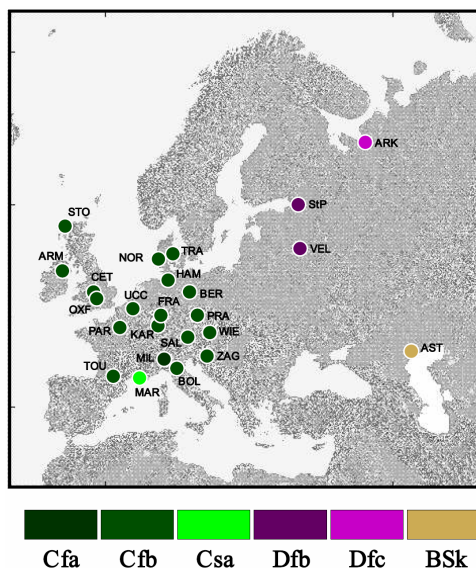


Figure 1. Geographical location of the 24 European stations with the daily air minimum and maximum temperature observations over more than a hundred years. Each location is color-coded in respect to the Köppen-Geiger climate classes [10] listed in Table 1.

Table 1. Geographical coordinates and the Köppen-Geiger climate class [10] of the 24 stations from ECA&D and the corresponding periods of the temperature series.

Station name	Abr	Class	Latitude, °N	Longitude, °E	Start	End
Armagh (UK)	ARM	Cfb	54.350	-6.650	1865	2001
Stornoway Airport (UK)	STO	Cfb	58.217	-6.317	1873	2001
Central England (UK)	CET	Cfb	52.417	-1.833	1881	2001
Oxford (UK)	OXF	Cfb	51.767	-1.267	1853	2001
Toulouse Blagnac (France)	TOU	Cfb	43.623	1.378	1878	2005
Paris Montsouris (France)	PAR	Cfb	48.823	2.337	1900	2001
Uccle (Belgium)	UCC	Cfb	50.800	4.350	1833	2001
Marseille Longchamp (France)	MAR	Csa	43.305	5.397	1900	2001
Karlsruhe (Germany)	KAR	Cfb	49.017	8.383	1876	2001
Nordby (Denmark)	NOR	Cfb	55.450	8.400	1874	2003
Frankfurt (Germany)	FRA	Cfb	50.117	8.667	1870	2001
Milan (Italy)*	MIL	Cfa	45.472	9.189	1838	2008
Hamburg Fuhlsbüttel (Germany)	HAM	Cfb	53.550	9.967	1879	2001
Tranebjerg (Denmark)	TRA	Cfb	55.850	10.600	1872	2003
Bologna (Italy)	BOL	Cfb	44.483	11.250	1814	2001
Salzburg (Austria)	SAL	Cfb	47.800	13.000	1874	2004
Berlin (Germany)	BER	Cfb	52.450	13.300	1876	2001
Praha Klementinum (Czech Republic)	PRA	Cfb	50.091	14.419	1775	2005
Zagreb Gric (Croatia)	ZAG	Cfb	45.817	15.978	1881	2001
Wien (Austria)	WIE	Cfb	48.233	16.350	1852	2004
St Petersburg (Russian Federation)	StP	Dfb	59.967	30.300	1881	2003
Velikie Lukie (Russian Federation)	VEL	Dfb	56.350	30.617	1881	2003
Arkhangelsk (Russian federation)	ARK	Dfc	64.500	40.733	1881	2003
Astrakhan (Russian Federation)	AST	BSk	46.283	46.283	1881	2003

Notes: (a) Cfa—warm temperate climate, fully humid, with hot summer; Cfb—warm temperate climate, fully humid, with warm summer; Csa—warm temperate climate with dry and hot summer; Dfb—snow climate, fully humid, with warm summer; Dfc—snow climate, fully humid, with cool summer and cold winter; BSk—cold steppe climate; (b) The two temperature series for Milan (ECA&D source IDs 105,247 for T_{\min} and 105248 for T_{\max} both starting in 1763) look suspiciously coherent, possibly, man-made before 1838.

pdf's are of classical use in climatology (see e.g. [5] and references therein).

An extensive list of indices has been proposed to characterize the climate at a given station from temperature, pressure, precipitation, etc recordings [6]. These are of course very useful. Nevertheless, we think that the patterns of the temperature statistics (the shapes of *pdf*'s, in particular) can provide much additional information allowing to characterize the “climate” at a given station at a single glance.

Note: We take the ECA&D non-blended series as they are, without submitting them to any kind of “homogeni-

zation” process. We think that such a process can hardly be applied to the data without a deep knowledge of the history of observations, which is particularly difficult to achieve for the old stations with long series of records. We prefer to trust the local observers whose diligent efforts on collecting and archiving the existing data is invaluable. Blind “homogenization” to a pre-conceptual model may lead to reject most of the data [7]: e.g., the homogeneity checking results for the 1901-2009 period (the ECA&D file TEMP_19012009_homogeneity.txt) found only 6 “*useful*”, 1 “*doubtful*”, and 118 “*suspect*” out of 122 stations.

It is well known that some stations, in particular, those installed in sites now included in a big city, can be affected by a heat island effect (e.g. [8]). We will point out some of them in the analysis.

3. The Empirical Distribution Functions

Let us start with taking all the daily minimum and maximum temperatures observed at the station of Bologna (BOL), ranked according to the calendar day and stacked. We consider successively the periods 1814-1970 and 1971-2000 (**Figures 2(a)** and **(b)**). The original readings of temperatures corresponding to the two periods for both T_{\min} (minimum daily temperature) and T_{\max} (maximum daily temperature) are in good agreement. Nevertheless, when averaging is applied, a slight increase in T_{\min} and T_{\max} for the months of December, January, February, and March, is noticeable (of the order of 1°C - 2°C). This might reflect the warming in Europe, in the last decade of the 20th century noted by *Le Mouél et al.* [9] to start actually in 1987.

We then compute and plot pf 's and pdf 's of T_{\min} and

T_{\max} with uniform bins $\Delta\tau = 1^{\circ}\text{C}$ at every station over successive periods of 30 years (and the remainder) depending on the length of the series in order to examine their long term evolution. **Figures 3-5** illustrate the results to follow.

First of all, we observe the striking stability of pf 's and pdf 's over time in all stations but those affected by a heat island effect: the T_{\min} and T_{\max} curves vary only slightly over a hundred years or more. However, the comparison of the temperature distributions derived from different 30-year intervals shows that these are hardly drawn from the same distribution. Specifically, **Figure 5** shows that for the two most recent intervals the difference between empirical probability distributions, $F_1(\tau) - F_0(\tau)$, may exceed +6% (T_{\min} at TRA and T_{\max} at MIL) indicating evident "warming" or go below -5% (T_{\max} at UCC) indicating evident "cooling". **Table 2** shows the results of the comparison of empirical distributions for each pair of time intervals at Prague (PRA), *i.e.* the longest ECA&D series of T_{\min} and T_{\max} . The two sample Kolmogorov-Smirnov statistic $\lambda_{K-S}(D, n, m) = [nm/(n + m)]^{1/2}D$, where

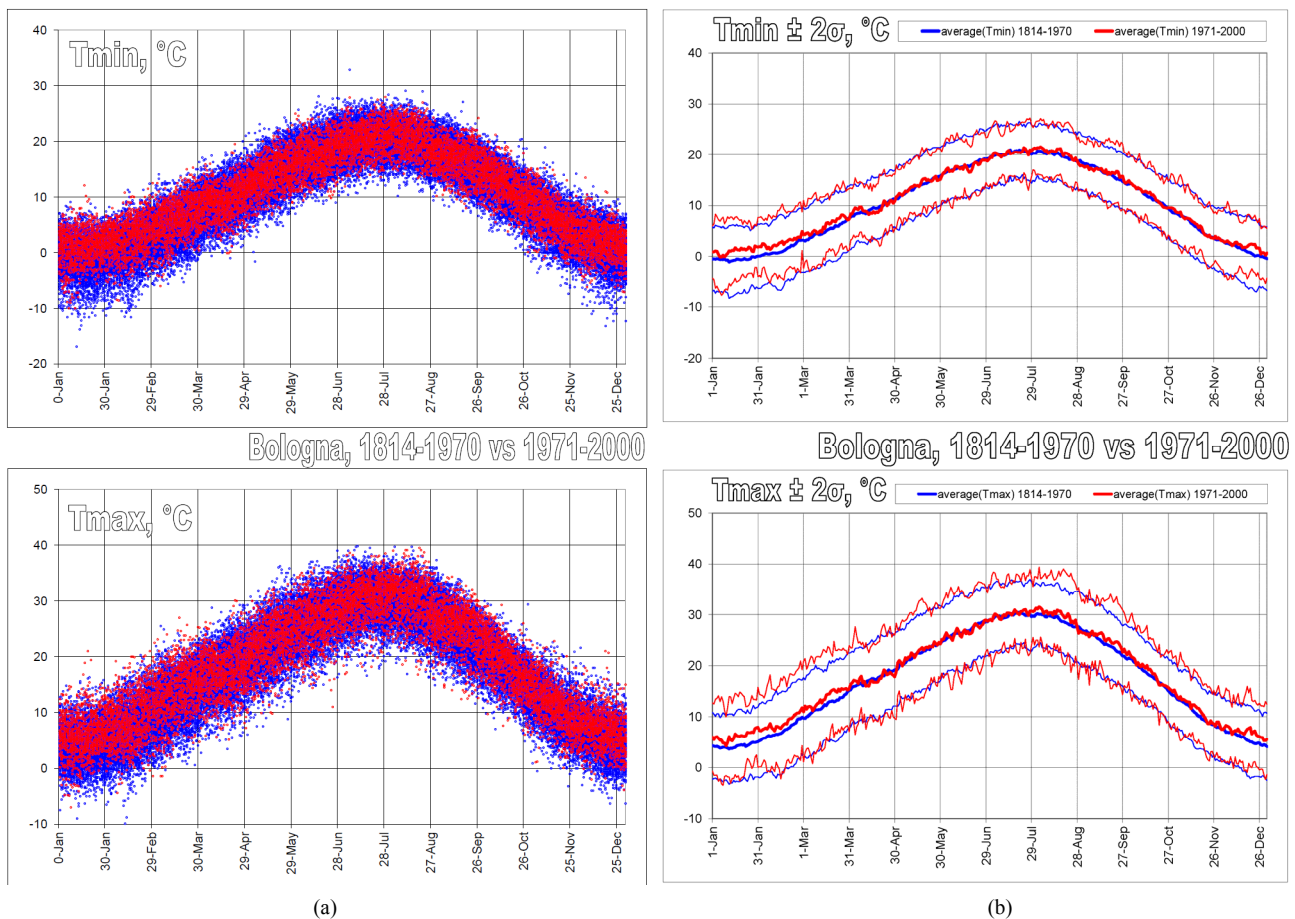


Figure 2. The daily minimum (left) and maximum (right) temperatures (a) and their averages (b) observed at Bologna on the calendar day in 1814-1970 (blue) and 1971-2000 (red). The graphs of averages are supplied with the plus/minus two standard deviation curves.

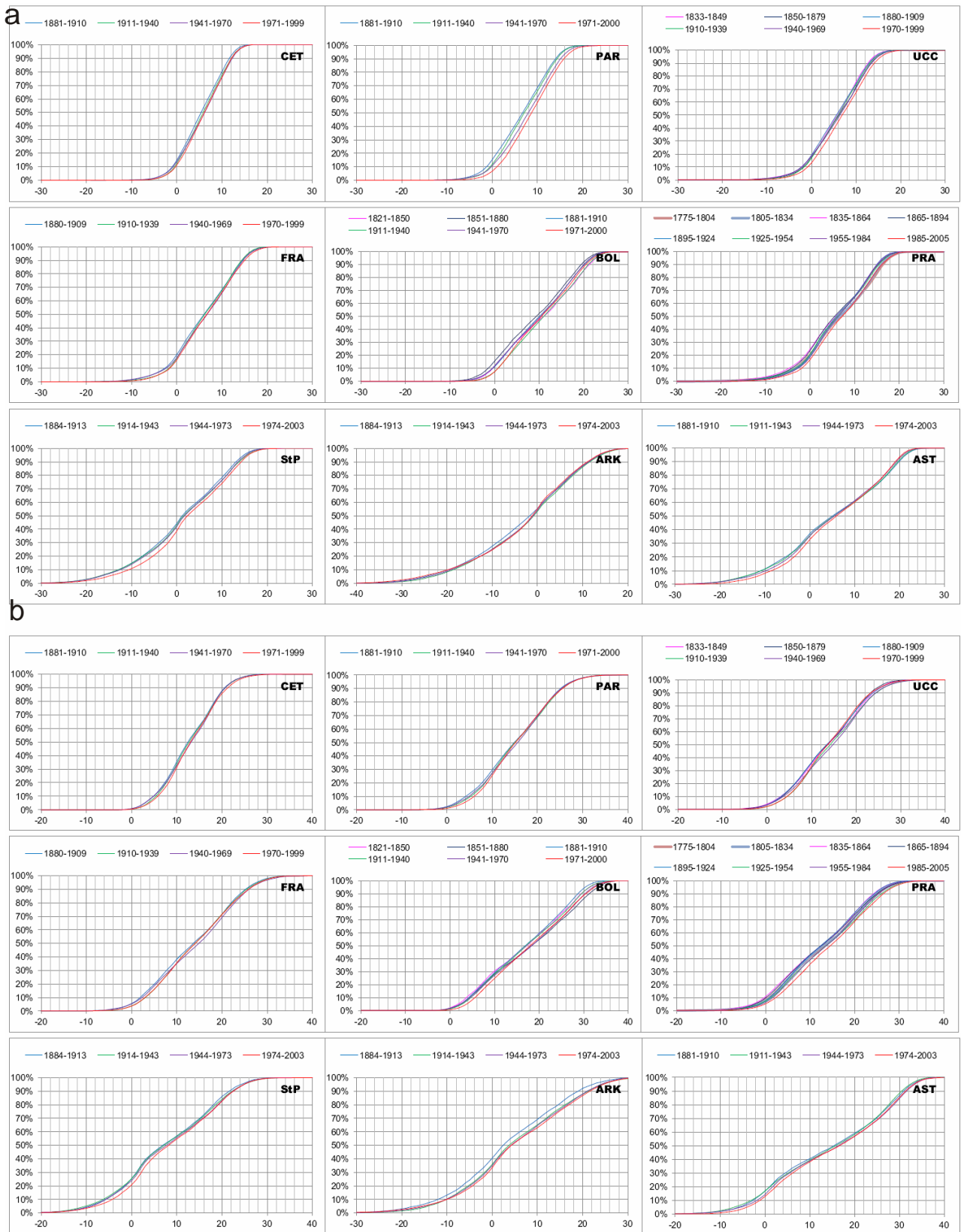


Figure 3. The empirical probability (distribution) functions, $F(\tau)$, of the minimum (a) and maximum (b) temperatures, T_{\min} and T_{\max} , over different time intervals. Note: the complete set of plots for the 24 European stations is given in Supplement.

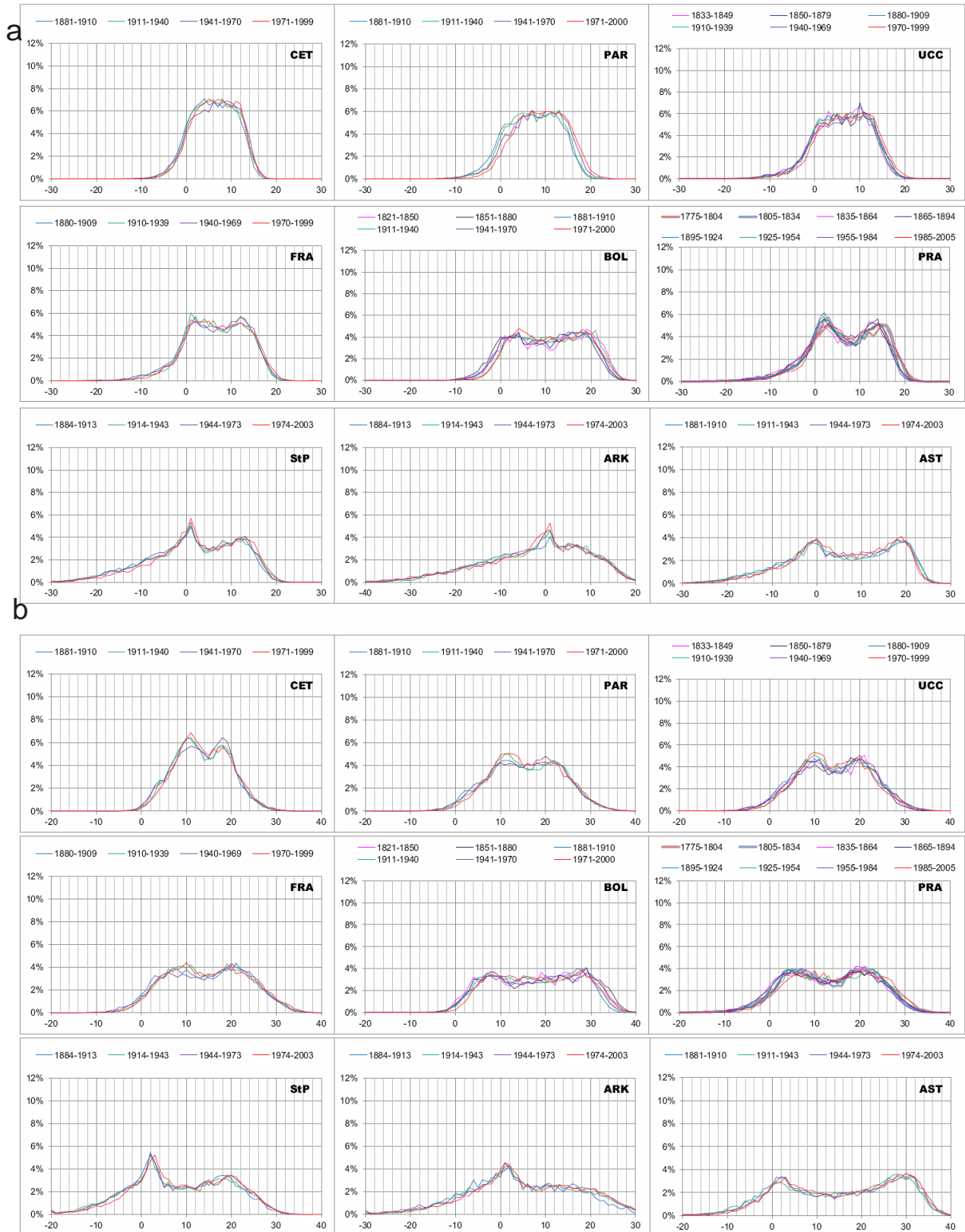


Figure 4. The empirical probability density (distribution) functions, $f(\tau)$, of the minimum (a) and maximum (b) temperatures, T_{\min} and T_{\max} , over different time intervals. Note: the complete set of plots for the 24 European stations is given in Supplement.

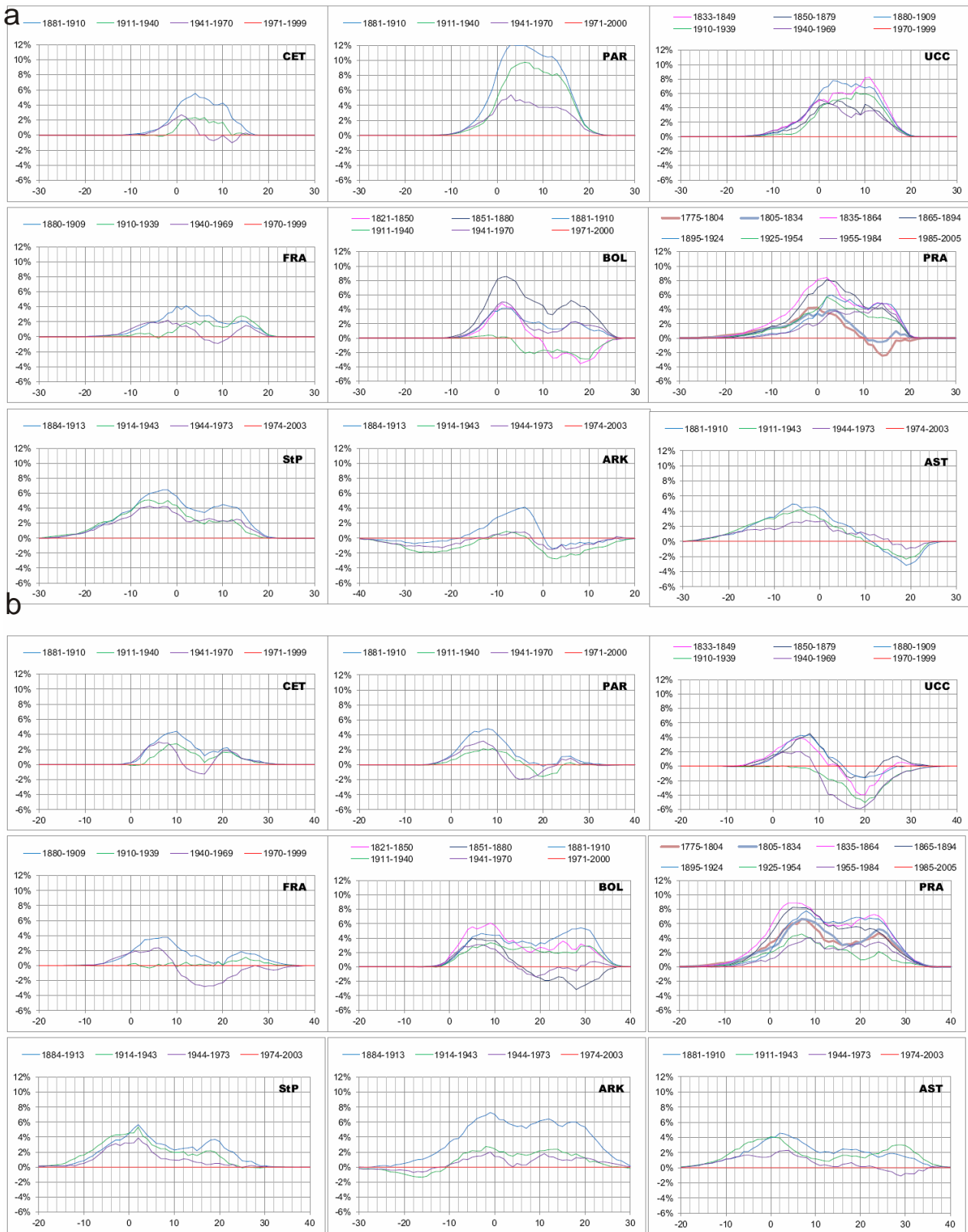


Figure 5. The difference between the empirical probability functions, $F(\tau)$, of the minimum (a) and maximum (b) temperatures, T_{\min} and T_{\max} , over different time intervals and the recent most one, $D_k(\tau) = F_k(\tau) - F_0(\tau)$. Note: $D_k(\tau) > 0$ indicates relative “warming”, while $D_k(\tau) < 0$ indicates relative “cooling”. The complete set of plots for the 24 European stations is given in Supplement.

Table 2. The K-S test comparison of 30-year intervals at Prague.

T _{min} at Prague (PRAHA-KLEMENTINUM; source-ID: 100079).								
	1775-1804	1805-1834	1835-1864	1865-1894	1895-1924	1925-1954	1955-1984	1985-2005.VI
	1	2	3	4	5	6	7	8
1	10957	-1.466	-5.371	-4.945	-5.350	-3.965	-5.432	-1.636
2	0.865	10957	-5.715	-4.968	-5.627	-3.582	-5.657	-0.548
3	0.142	0.048	10958	-1.105	-0.321	-0.007	-0.061	0.000
4	0.263	0.182	0.958	10957	-1.094	-0.095	-0.487	-0.012
5	1.108	0.994	3.451	2.574	10957	-0.676	-0.082	-0.002
6	0.574	0.325	2.998	2.195	1.527	10957	-1.467	0.000
7	1.879	1.530	4.593	3.791	1.948	1.941	10958	-0.020
8	2.819	4.108	5.609	5.417	3.977	3.814	3.247	7425

T _{max} at Prague (PRAHA-KLEMENTINUM; source-ID: 100081).								
	1775-1804	1805-1834	1835-1864	1865-1894	1895-1924	1925-1954	1955-1984	1985-2005.VI
TX	1	2	3	4	5	6	7	8
1	10957	-0.946	-2.573	-1.709	-2.608	0.000	0.000	0.000
2	0.703	10957	-4.632	-3.191	-4.089	0.000	-0.280	0.000
3	0.115	0.010	10958	-0.077	-0.795	0.000	0.000	0.000
4	0.277	0.869	1.656	10957	-1.344	-0.047	-0.007	0.000
5	0.912	1.146	2.620	1.756	10957	-0.405	-0.020	-0.006
6	2.027	3.468	4.345	3.344	4.344	10957	-1.630	-0.006
7	2.326	3.280	4.526	3.811	2.873	0.872	10958	-0.019
8	4.421	6.946	5.896	5.503	5.166	3.037	2.710	7425

Note: the sample size of a 30-year interval is given on the diagonal, while the values of λ_{KS-} and λ_{KS+} are put above and below the diagonal, respectively. The λ_{KS-} and λ_{KS+} above 1.36 in absolute value are highlighted (see text).

$D = \max |F_i(\tau) - F_j(\tau)|$ is the maximum value of the absolute difference between the empirical distributions $F_i(\tau)$ and $F_j(\tau)$ of the two samples (τ covers the entire range of temperature index $T = T_{\min}$ or T_{\max}), whose sizes are n and m respectively. **Table 2** summarizes the test results in terms of λ_{K-S} , leaving the issue of statistical significance in terms of probability to more delicate testing against randomized data [3]. For the purpose of further comparison, we distinguish the two possible outcomes of the Kolmogorov-Smirnov test by providing in **Table 2** both extremes, *i.e.* the minimum λ_{K-S-} and maximum λ_{K-S+} of $(F_i(\tau) - F_j(\tau))$. We see that the maximum of the absolute values of λ_{K-S-} and λ_{K-S+} are above the standard critical value of 1.36 (highlighted) for all pairs of intervals considered for Prague. This is a clear indication of intrinsic variability of local “climate”, however quite small at the time scale of a few decades, which in detail analysis requires an accurate application of specially designed problem oriented statistical tools (e.g. [3]). In this

respect it is notable that for Bologna (**Figure 5**, BOL) the most recent interval (1971-2000), at the same time, is “cooler” in terms of T_{\min} and “warmer” in terms of T_{\max} than in the same one 30-year period (1911-1940) in the past. There are also cases of a Z-shape differences of pf s with a “warming” at low temperatures and “cooling” at high temperatures, like for T_{\max} in Paris and Uccle (**Figure 5(b)**, PAR and UCC).

On the contrary, the shape patterns of pf s and pdf s change quite significantly from one station to the other (**Figures 3** and **4**). The sets of diagrams obtained for all 24 stations are self-explanatory and provide a lot of synthetic information on the European temperatures in space and time. In particular, we will show now that the shape patterns of pf s and pdf s can be organized into three distinct groups corresponding to the different regions of Europe with different climates (**Figure 1**).

a) The 4 stations located in the Russian Federation (Arkhangelsk, St Petersburg, Velikie Lukie, Astrakhan)

share the trait of having a harsh continental climate.

In Arkhangelsk, situated close to the polar circle, the winters are very long and cold and the summers are short and cool or moderately warm. Over the century, the than probability curves (pf 's) show an overall warming of less 2°C for negative T_{\min} and about 2°C for almost the entire range of T_{\max} (Figures 3(a) and (b)). Note that the over-

all warming is essentially attributed to transition from 1884-1913 to 1914-1943, while the pf 's for the remaining three intervals are much closer to each other for both T_{\min} and T_{\max} . The probability density curves for T_{\max} and T_{\min} (Figures 4(a) and (b)) exhibit a peak around 0°C , with a long heavy tail towards colder temperatures and a shoulder at higher temperatures (3°C to 10°C for T_{\min} and

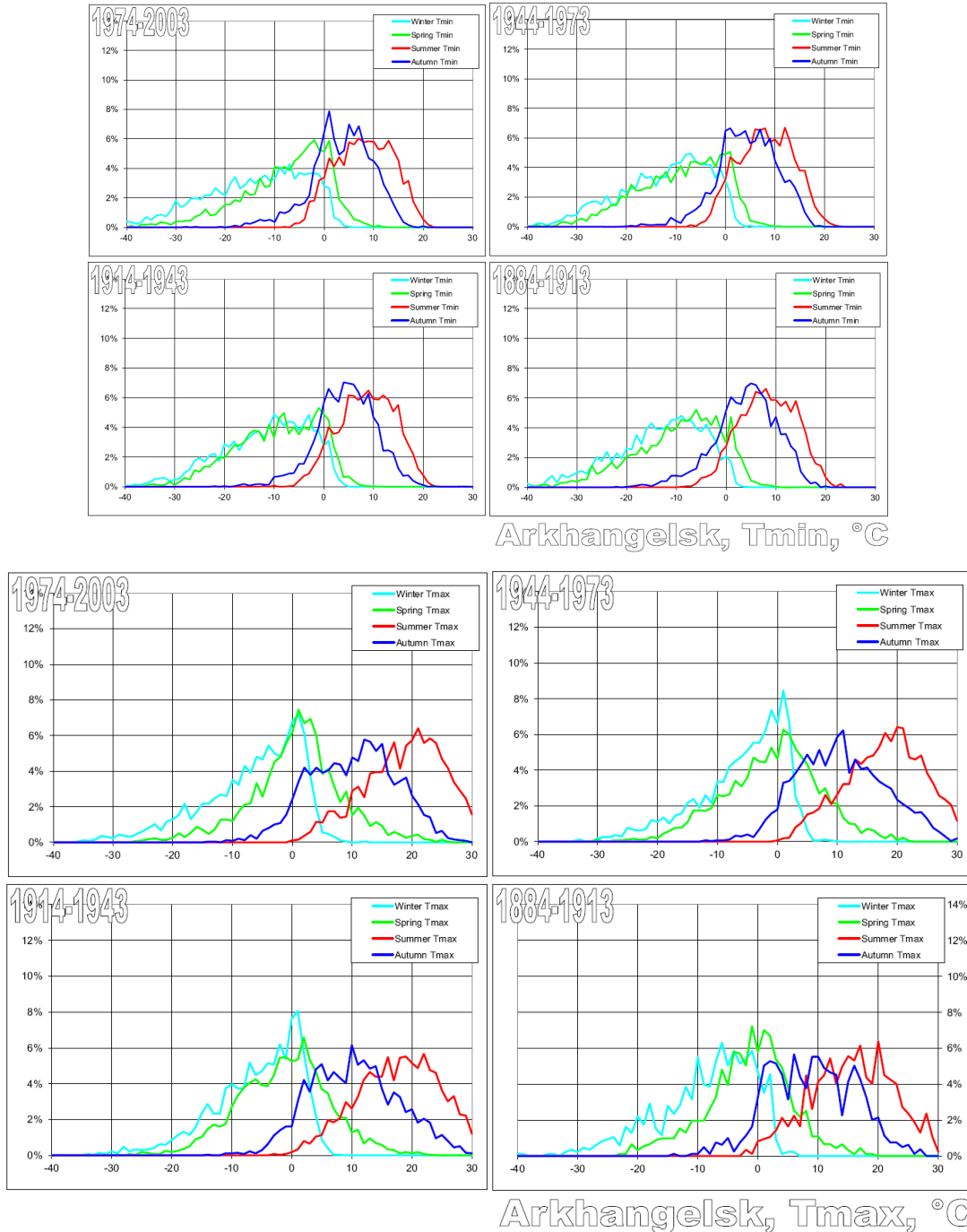


Figure 6. The four-seasons' probability density curves, $f(\tau)$, for T_{\min} (a) and T_{\max} (b) in Arkhangelsk. Note: the four seasons are defined as follows: winter = November 7-February 5, spring = February 6-May 7, summer = May 8-August 7, August 8-November 6.

5°C to 20°C for T_{max} (Figures 3(c) and (d)).

Probability density curves were drawn separately for the four seasons (Figure 6). The T_{min} and T_{max} curves for winter and spring are similar and they both exhibit a long heavy tail towards lower temperatures, probably due to the persistence of the snow cover. The curves for autumn and summer are also similar after a translation. The high proportion of T_{min} for autumn and summer and T_{max} for winter and spring close to 0°C accounts for the strong peak in the stacked yearly curves.

St Petersburg and Velikie Lukie are both in a snow zone of continental climate, but more to the south than Arkhangelsk. Although the temperatures are less cold than in Arkhangelsk, the yearly curves (Figure 4) still exhibit a strong peak around 0°C and a long tail towards colder temperatures. However, there are more warm days in autumn and summer and the curves exhibit an uplifted shoulder with a distinct peak above 10°C for T_{min} and up to 20°C for T_{max} .

In Astrakhan, one of the driest cities in Europe, on the northern shore of the Caspian Sea, the steppe climate is continental and the pdf curves exhibit again a long heavy tail towards lower temperatures. The presence of two well-identified peaks at temperatures around 0°C and 20°C for T_{min} (Figure 4(a)) and 30°C for T_{max} (Figure 4(b))

accounts for cold winters and hot summers much warmer than in St Petersburg or Velikie Lukie.

b) In central Europe (Berlin, Hamburg, Prague, Frankfurt, Karlsruhe, Wien, Salzburg, Zagreb, Milan, Bologna), the climate is mild continental with no dry season, not as harsh as in Russia.

A typical example is Prague (Figure 7) where T_{min} and T_{max} temperatures have been observed since 1775. The T_{min} and T_{max} pdf's (Figure 4) for the periods 1775-1804, 1805-1834, 1835-1864, 1865-1894, 1895-1924, 1925-1954, 1955-1984, and 1985-2005, are not very different, they exhibit two distinct peaks above 0 and below 15°C for T_{min} and around 5°C and 20°C for T_{max} . The T_{min} curves for spring and autumn are not far apart from those for winter and summer, respectively (Figure 7(a)), but the T_{max} curves for spring and summer are more clearly shifted towards temperatures higher by up to 10°C with respect to those for winter and autumn (Figure 7(b)). Although of a character somewhat transitional to that of Western Europe, Karlsruhe, Frankfurt and Bologna (Figure 8) can be, for simplicity sake, put together with the stations of central Europe.

c) In Western Europe (Stornoway, Armagh, Central England, Oxford, Tranebjerg, Nordby, Uccle, Paris, Toulouse, Marseille), the climate is frankly oceanic, warm-

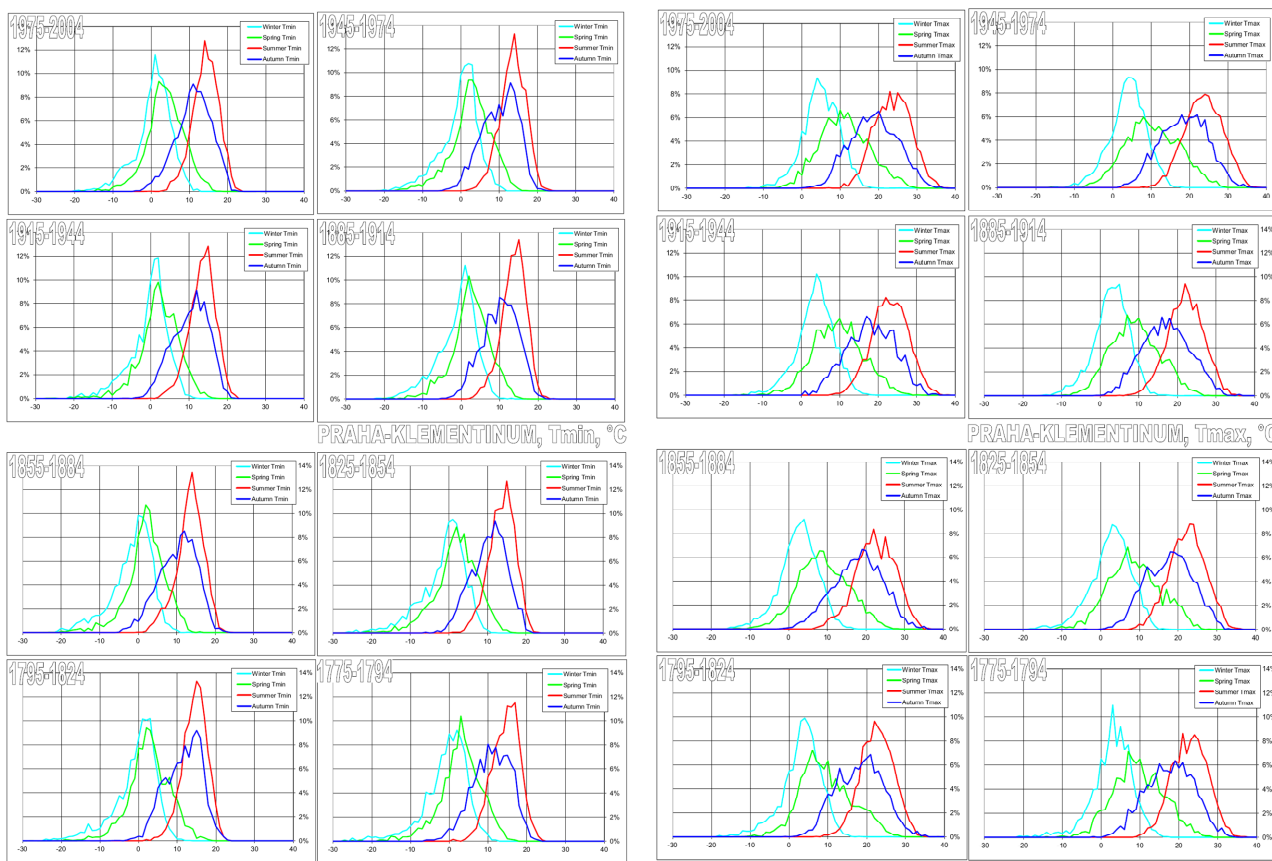
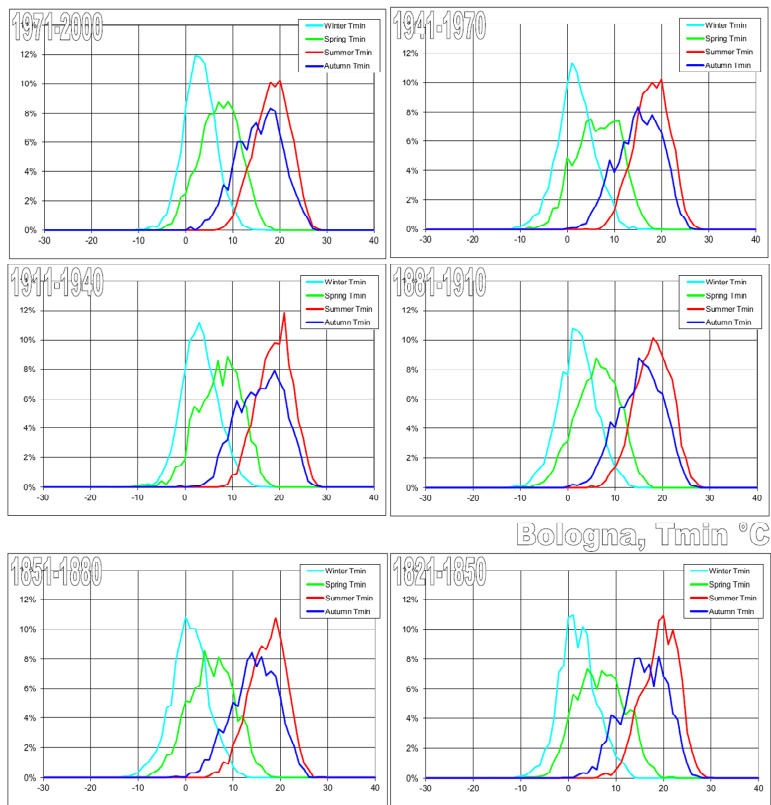
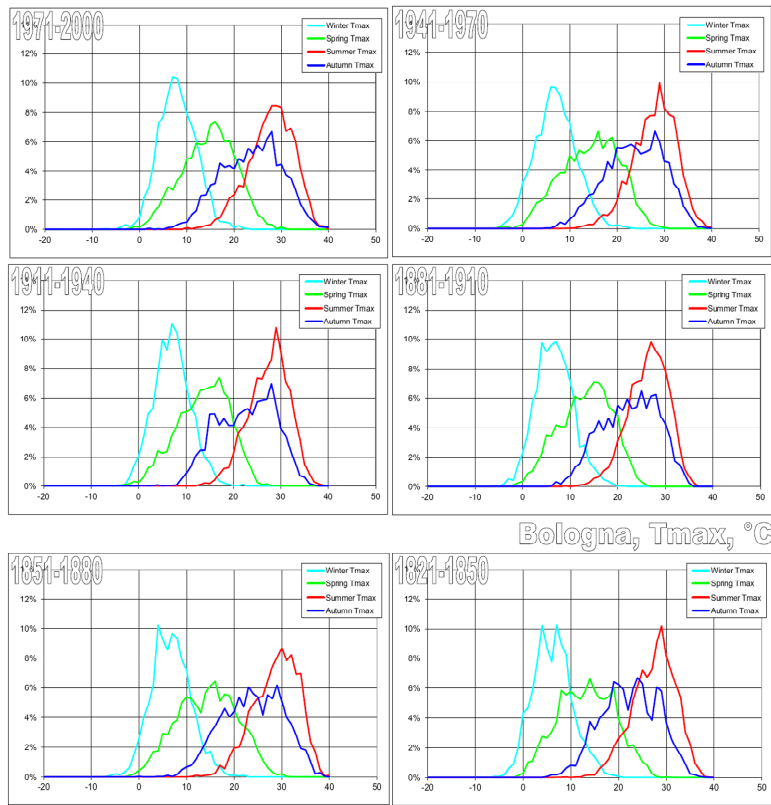


Figure 7. The four-seasons' probability density curves, $f(\tau)$, for T_{min} (a) and T_{max} (b) in Prague. Note: same as in Figure 6.



Bologna, T_{min} °C

(a)



Bologna, T_{max} , °C

(b)

Figure 8. The four-seasons' probability density curves, $f(t)$, for T_{min} (a) and T_{max} (b) in Bologna. Note: same as in Figure 6.

fully humid with warm summer, except for Marseille with dry and hot summer. The peaks of *pdf*'s now overlap yielding a single wide peak at about 10°C for T_{\min} and an almost flat plateau from 10°C to above 20°C for T_{\max} (**Figure 4**). A typical example is Paris.

4. Temperature Changes

From the comparison of repartition *pf* and *pdf* curves, it is possible to obtain an estimate of the average temperature changes over successive 30 years period, for the various stations. We just give a brief account of it.

a) At Arkhangelsk and St Petersburg (as already mentioned above for Arkhangelsk, **Figure 3**) the average T_{\max} is higher for about 2°C for the three 30 years periods starting in 1914, as compared with the period 1884-1913.

There is no significant difference between the periods 1914-1943, 1944-1973, 1974-2003. T_{\min} does not significantly vary from 1884 to 2003. Although somewhat less clearly, T_{\min} and T_{\max} at Velikie Lukie and Astrakhan exhibit a similar behavior.

b) At Prague (Praha-Klementium), there is no discernible difference between the 30-year period curves for T_{\max} starting in 1775 up to 1985. The curve for 1985-2005 shows a temperature increase of about 1°C or more. There is a slighter increase in T_{\min} , moreover, the curves for 1775-1804 and 1805-1834 show up about the same or even higher temperatures in the upper quartiles of the distributions. The temperatures at Salzburg, Wien, Karlsruhe and Bologna behave approximately in the same way. At Nordby and Tranebjerg, although all the curves are somewhat bundled together, there may be a slight increase in both T_{\min} and T_{\max} over the last 30-year period.

At Zagreb, as well as at Berlin, and less clearly at Hamburg and Frankfurt, there is no discernible evolution of T_{\min} and T_{\max} since the 1880's.

c) At the stations situated in the British Isles (Oxford, Central England, Armagh), except for the northern most one (Stornoway) there is practically no change of either T_{\max} or T_{\min} over the whole period 1853-1972, then, in the last interval 1973-2001) a small warming of about 0.5°C is observed (see *Le Mouël et al.*, 2009).

d) At Uccle, Toulouse, and very clearly at Paris and Marseille, it is T_{\min} that increases over the last 30 years, while T_{\max} behaves differently—decreases for about 1°C at Uccle, increases for about 1°C at Toulouse, and does not change that much at Paris and Marseille. This could be attributed, at least partly, to a heat island effect, as the cities of Brussels (close to Uccle), Toulouse, Paris, and Marseille have considerably expanded in the last 30 years.

5. Quantitative Climate Classifications

We have identified above three climatic regions, for

which the shape of the *pf* and *pdf* curves is similar: Eastern Europe, Central Europe, and Western Europe. We will now retrieve this classification, in its broad lines, through quantitative criteria.

Entropy is a measure of uncertainty or diversity of the system. It characterizes also the quantity of information—taken in average—which is missing for knowing whether state i (here a temperature in the interval from T_i to $T_i + \Delta T$) will be realized when only the *pdf* is known. Specifically, we compute the Shannon's entropy H defined as $H = -\sum p_i \ln p_i$, where p_i is the probability density function, $i = 1, \dots, N$. The maximum $H = \ln N$ is reached for the uniform distribution $p_i = 1/N$ (for all i), therefore, for the sake of comparison, we use here normalized value $H^* = H/\ln N$ (i.e., the so-called, *efficiency* in information theory).

In **Figure 9** the color of the observatory site depends on the value of H^* determined for the T_{\min} *pdf*'s within a 60°C range split into 1°C bins. At the 24 European stations considered the value of H^* ranges from the maximum of 0.926 at Arkhangelsk (Russia) to the minimum of 0.684 at Stornoway Airport (Scotland). The same as abovementioned three groups of the European climate zones can be obtained by setting the two boundary thresholds of $H^*_{T_{\min}} = 0.75$ and 0.85. In a similar way the classification of climatic regions could be obtained by using the Shannon's entropy based on T_{\max} (see **Table 3**); specifically, the same three groups (though with a slightly different order of stations in a group) can be distinguished by setting the boundary thresholds $H^*_{T_{\max}}$ at 0.8 and 0.9. Moreover, additional boundary thresholds (e.g. $H^*_{T_{\min}} = 0.77$ and 0.81 or $H^*_{T_{\max}} = 0.81$ and 0.87) allow further details of classification that are not present in the classical one [10], which attributes three quarters of the sites considered to the same class Cfb, i.e. warm zone fully humid with warm summer.

Cluster analysis provides another approach to a quantitative classification of climatic zones. It is illustrated with an application of single link cluster analysis of the correlations between the temperature *pdf*'s. **Figure 10** combines the two symmetric matrices of the correlation coefficients between all the pairs of *pdf*'s at different stations computed for T_{\min} (values below the diagonal) and T_{\max} (values above the diagonal) leaving empty the 100% diagonal. To simplify the visual perception of the pair correlations, their values are given on a color coded background.

Figure 11 displays the dendrograms resulting from single link cluster analyses of the correlation matrices for the distributions of T_{\min} and T_{\max} given in **Figure 10**. Each horizontal segment on a dendrogram represents a link between the two clusters indicated by vertical segments. The level of similarity of a link is given by the value of correlation shown on the ordinate axis (note that

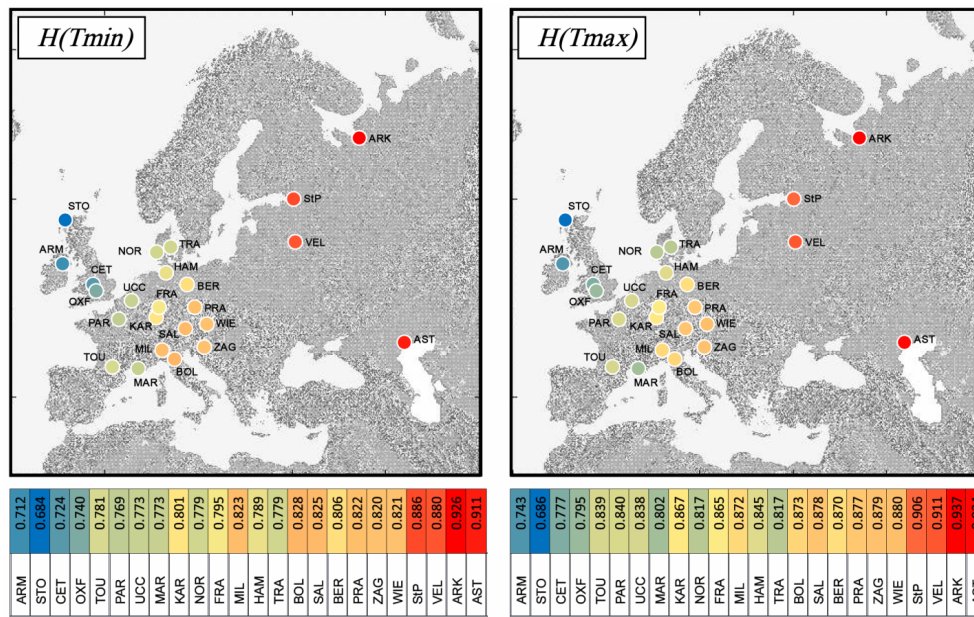


Figure 9. The normalized Shannon’s entropy H^* for T_{min} (left) and T_{max} (right) at the 24 European stations.

Table 3. The normalized Shannon’s entropies H^* computed from T_{min} and T_{max} .

Location	$H^*_{T_{min}}$	$H^*_{T_{max}}$	Order by $H^*_{T_{min}}$ and $H^*_{T_{max}}$	
STO—Stornoway airport (UK)	0.684	0.686	1	1
ARM—Armagh (UK)	0.712	0.743	2	2
CET—Central England (UK)	0.724	0.777	3	3
OXF—Oxford (UK)	0.740	0.795	4	4
PAR—Paris, (France)	0.769	0.840	5	10
MAR—Marseille (France)	0.773	0.802	6	5
UCC - Uccle (Belgium)	0.773	0.838	7	8
NOR—Nordby (Denmark)	0.779	0.817	8	6
TRA—Tranebjerg (Denmark)	0.779	0.817	9	7
TOU—Toulouse (France)	0.781	0.839	10	9
HAM—Hamburg (Germany)	0.789	0.845	11	11
FRA—Frankfurt (Germany)	0.795	0.865	12	12
KAR—Karlsruhe (Germany)	0.801	0.867	13	13
BER—Berlin (Germany)	0.806	0.870	14	14
ZAG—Zagreb Gric (Croatia)	0.820	0.879	15	19
WIE—Wien (Austria)	0.821	0.880	16	20
PRA—Prague (Czech Republic)	0.822	0.877	17	17
MIL—Milan (Italy)	0.823	0.872	18	15
SAL—Salzburg (Austria)	0.825	0.878	19	18
BOL—Bologna (Italy)	0.828	0.873	20	16
VEL—Velikie Lukie (Russia)	0.880	0.911	21	22
StP—St Petersburg (Russia)	0.886	0.906	22	21
AST—Astrakhan (Russia)	0.911	0.934	23	23
ARK—Arkhangelsk (Russia)	0.926	0.937	24	24

levels increase downwards). For example, the link, above which a single cluster of the 24 stations is achieved, corresponds to a similarity level of 86.0% for T_{min} (Figure 11(a)) and 78.4% for T_{max} (Figure 11(b)). For T_{min} , there are four clusters at a level of similarity above 95%: these are Astrakhan (AST), Milan and Bologna (MIL, BOL), Arkhangelsk (ARK), and the remaining 20 of the 24 stations. A level above 99.7% (*i.e.* the maximum of the values below the diagonal in Figure 10) delivers the split into 24 classes including each single station by breaking the highest correlation link between Karlsruhe (KAR) and Frankfurt (FRA). For T_{max} , the level of similarity above 90% provides separation into four clusters: these are Astrakhan (AST), Arkhangelsk (ARK), St Petersburg and Velikie Lukie (StP, VEL), and the remaining 20 European stations. The level of 95% splits two additional clusters: Stornoway (STO) and Toulouse and Marseille (TOU, MAR). A level above 99.4% (*i.e.* the maximum of the values above the diagonal in Figure 10) is needed to break all the T_{max} correlation links between the 24 stations.

6. Conclusions

The study of the statistical distribution of daily minimum and maximum temperatures in 24 European stations, from long series of more than a century, reveals two simple traits: a strong stability of the distributions at the different stations during the whole time span available; a strong, but ordered along a general trend, variability in space.

In the Eastern European stations, one notices an increase of about 2°C of the maximum temperatures in the

TN\TX	ARM	STO	CET	OXF	TOU	PAR	UCC	MAR	KAR	NOR	FRA	MIL	HAM	TRA	BOL	SAL	BER	PRA	ZAG	WIE	StP	VEL	ARK	AST
ARM		90.5%	97.3%	96.0%	74.9%	85.4%	88.4%	59.8%	79.6%	85.1%	79.6%	63.1%	87.2%	81.2%	62.0%	74.2%	77.6%	72.4%	64.1%	69.4%	54.4%	48.8%	32.5%	21.1%
STO	99.1%		85.5%	82.2%	58.7%	71.0%	74.2%	42.8%	65.4%	75.3%	66.2%	53.7%	73.8%	70.2%	53.2%	59.9%	63.9%	58.5%	50.0%	54.3%	42.9%	33.9%	32.3%	15.7%
CET	98.1%	95.9%		98.8%	79.1%	91.4%	94.8%	63.2%	87.1%	89.4%	87.4%	69.4%	93.0%	86.7%	68.4%	82.1%	85.4%	80.8%	72.5%	78.3%	61.2%	57.6%	35.6%	28.0%
OXF	98.1%	95.0%	99.0%		85.1%	95.3%	96.8%	69.7%	90.6%	86.1%	90.3%	73.6%	92.9%	85.1%	72.0%	85.4%	87.7%	83.8%	78.0%	82.7%	62.0%	60.7%	33.2%	32.1%
TOU	85.9%	80.6%	89.6%	92.6%		93.9%	85.9%	95.9%	88.7%	62.0%	84.9%	85.9%	75.0%	61.0%	85.1%	82.2%	77.9%	77.4%	88.8%	82.8%	44.2%	51.2%	7.1%	52.1%
PAR	90.1%	85.0%	93.8%	96.2%	98.8%		97.8%	81.7%	97.3%	79.7%	95.8%	85.8%	90.7%	80.0%	84.2%	92.2%	91.5%	90.2%	91.1%	92.0%	61.1%	65.3%	25.7%	48.3%
UCC	95.5%	91.5%	98.3%	99.0%	94.2%	97.4%		70.8%	97.3%	88.7%	97.6%	82.4%	96.8%	89.2%	80.7%	94.0%	95.7%	93.4%	88.0%	92.7%	69.1%	70.9%	36.5%	45.6%
MAR	72.3%	67.1%	75.6%	79.9%	95.8%	91.2%	81.4%		76.6%	46.5%	71.7%	80.6%	59.2%	44.3%	80.3%	71.1%	63.6%	64.4%	82.6%	72.0%	31.6%	40.6%	-8.2%	52.4%
KAR	89.5%	84.3%	93.4%	95.3%	95.5%	97.3%	98.0%	84.4%		84.7%	99.4%	90.8%	94.0%	86.1%	88.7%	98.0%	97.3%	97.0%	96.1%	97.8%	70.7%	75.5%	35.9%	61.2%
NOR	91.4%	86.8%	95.4%	96.0%	90.5%	94.6%	98.3%	76.0%	98.2%		87.7%	68.0%	96.6%	98.4%	66.1%	86.9%	91.1%	87.7%	72.2%	82.2%	77.9%	73.7%	56.5%	40.0%
FRA	89.8%	84.9%	93.6%	95.5%	95.9%	97.9%	97.9%	85.5%	99.7%	98.1%		89.6%	95.8%	89.4%	87.4%	98.5%	98.6%	98.3%	94.7%	97.9%	73.5%	77.6%	39.5%	60.2%
MIL	68.0%	64.0%	70.4%	73.5%	87.2%	82.4%	76.2%	90.8%	81.9%	75.0%	82.8%		77.4%	68.1%	99.3%	88.2%	84.4%	86.1%	95.1%	88.5%	49.8%	57.7%	14.7%	78.4%
HAM	93.4%	89.5%	96.8%	97.1%	91.5%	95.2%	99.1%	77.3%	98.4%	99.5%	98.4%	76.0%		97.4%	75.2%	94.3%	97.4%	94.7%	83.5%	91.5%	79.7%	78.8%	52.2%	47.0%
TRA	91.7%	87.7%	95.1%	95.0%	87.3%	91.8%	97.4%	71.6%	96.9%	99.2%	96.5%	73.1%	99.2%		65.3%	89.5%	93.9%	91.0%	74.5%	85.6%	84.2%	81.1%	62.8%	43.5%
BOL	67.0%	63.0%	69.4%	72.2%	85.5%	80.7%	74.6%	89.4%	79.6%	73.2%	80.5%	99.4%	74.1%	71.2%		85.1%	81.6%	83.0%	92.8%	85.4%	44.4%	52.2%	11.3%	78.3%
SAL	86.3%	81.0%	90.4%	92.0%	89.2%	92.1%	95.7%	75.1%	98.1%	97.8%	97.2%	75.3%	97.8%	97.8%	72.6%		98.7%	99.3%	95.8%	99.3%	80.4%	84.9%	47.3%	65.4%
BER	90.4%	85.8%	93.9%	94.9%	90.9%	94.0%	97.7%	77.2%	98.9%	99.1%	98.5%	77.8%	99.4%	99.1%	75.5%	99.2%		99.2%	91.6%	97.7%	82.2%	84.9%	52.0%	60.0%
PRA	82.1%	76.6%	86.1%	89.0%	93.6%	94.3%	92.7%	85.6%	97.9%	94.8%	98.2%	86.1%	94.5%	92.8%	83.4%	95.7%	96.2%		93.8%	99.0%	81.7%	86.0%	49.8%	63.6%
ZAG	74.0%	67.9%	78.5%	82.5%	95.1%	92.1%	86.7%	93.0%	93.5%	86.8%	93.7%	92.7%	87.2%	84.2%	90.0%	89.4%	89.6%	96.8%		97.0%	66.3%	74.8%	28.0%	74.6%
WIE	80.8%	74.7%	85.2%	88.4%	93.5%	94.0%	92.6%	85.1%	98.1%	94.6%	97.9%	85.4%	94.3%	92.9%	82.5%	96.8%	96.5%	99.5%	97.0%		78.7%	84.8%	44.5%	67.2%
StP	75.7%	70.4%	80.0%	81.4%	78.0%	81.1%	86.5%	62.7%	90.4%	90.4%	88.9%	64.1%	90.5%	90.8%	60.4%	95.8%	93.2%	89.2%	81.9%	90.9%		97.9%	89.5%	50.4%
VEL	81.7%	77.9%	85.4%	85.1%	75.9%	80.5%	88.9%	57.7%	89.2%	91.3%	87.5%	58.5%	92.0%	92.9%	55.1%	95.2%	93.4%	84.3%	75.4%	86.2%	97.5%		80.3%	58.4%
ARK	69.7%	68.6%	71.0%	68.8%	50.7%	57.8%	71.5%	28.1%	70.3%	75.4%	68.1%	37.7%	76.6%	78.3%	37.5%	79.6%	77.8%	64.0%	49.8%	65.6%	88.6%	92.8%		40.8%
AST	49.0%	44.7%	51.6%	54.4%	67.1%	61.4%	60.2%	68.1%	69.2%	62.9%	67.7%	86.0%	63.5%	62.8%	85.1%	70.4%	68.6%	74.7%	80.9%	76.3%	71.2%	63.6%	52.6%	

Figure 10. The correlations between the minimum daily temperature empirical density functions at different stations (below the diagonal); same for the maximum daily temperature (above the diagonal). To facilitate visual perception the correlation values are given on the color-coded background.

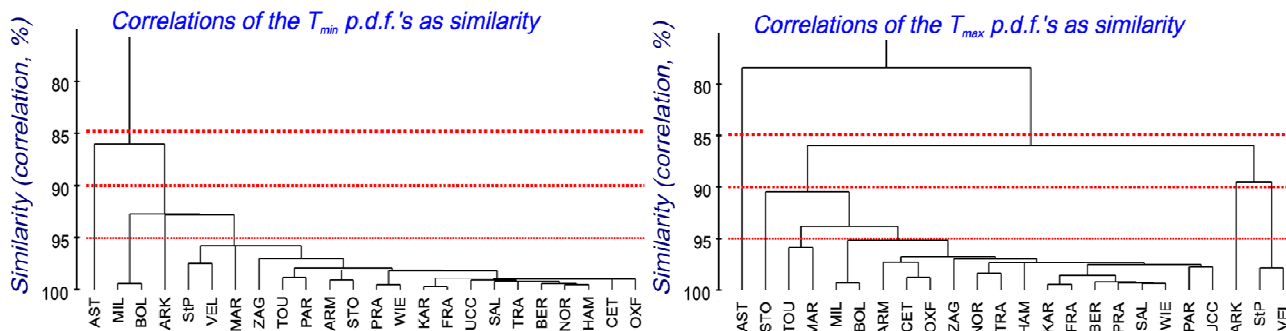


Figure 11. The results of a single-link cluster analysis based on correlation of the daily temperature density functions as the measure of similarity (upper plate for T_{min} and lower plate for T_{max}). The arbitrary levels of 85%, 90%, and 95% correlation marked with the dash-lines.

last 30 years with respect to the preceding time spans, while in Central Europe there is an increase of about 1°C of the maximum temperatures at some stations, and no discernible increase at the others. In Western Europe (British Isles, Belgium, and France) there is generally no discernible increase or decrease of the maximum and the minimum temperatures along the last century. The warming of some 0.6°C observed in the last decade of the 20th century [9], is hardly visible in our analysis based of 30-year intervals. At big cities' stations (Paris, Marseille, Toulouse, Brussels) however, there is a noticeable increase of the minimum temperature, probably due to a heat island effect.

It is verified that there are several distinct stable climatic regions in Europe, which is a common knowledge; nevertheless, in each of them there is some variability in time at each station as attested by the Kolmogorov-Smirnov test, and larger variability from station to station. The classification in climatic zones can be made by a naked eye comparison of the *pf* and *pdf* curves, which contain a lot of information. It can be corroborated by quantitative analysis of those functions based on the Shannon entropy or cluster analysis, used separately or in combination. Such objective methods, as well as other tools of pattern recognition, could be employed for a more widespread and systematic classification of climatic zones.

REFERENCES

- [1] A. M. G. Klein Tank, *et al.*, "Daily Dataset of 20th-Century Surface Air Temperature and Precipitation Series for the European Climate Assessment," *International Journal of Climatology*, Vol. 22, 2002, pp. 1441-1453.
- [2] J.-L. Le Mouél, V. Kossobokov and V. Courtillot, "A Solar Pattern in the Longest Temperature Series from Three Stations in Europe," *Journal of Atmospheric and Solar-Terrestrial Physics*, Vol. 72, 2010, pp. 62-76. [doi:10.1016/j.jastp.2009.10.009](https://doi.org/10.1016/j.jastp.2009.10.009)
- [3] V. Kossobokov, J.-L. Le Mouél and V. Courtillot, "A Statistically Significant Signature of Multi-Decadal Solar Activity Changes in Atmospheric Temperatures at Three European Stations," *Journal of Atmospheric and Solar-Terrestrial Physics*, Vol. 72, 2010, pp. 595-606. [doi:10.1016/j.jastp.2010.02.016](https://doi.org/10.1016/j.jastp.2010.02.016)
- [4] D. E. Parker, T. P. Legg and C. K. Folland, "A New Daily Central England Temperature Series, 1772-1991," *International Journal of Climatology*, Vol. 12, 1992, pp. 317-342. [doi:10.1002/joc.3370120402](https://doi.org/10.1002/joc.3370120402)
- [5] W. J. Burroughs, "Climate Change: A Multidisciplinary Approach," 2nd Edition, Cambridge University Press, Cambridge UK, 2007, 390 p. [doi:10.1017/CBO9780511803819](https://doi.org/10.1017/CBO9780511803819)
- [6] A. van Engelen, A. Klein Tank, G. van de Schrier and L. Klok, "Towards an Operational System for Assessing Observed Changes in Climate Extremes," European Climate Assessment & Dataset (ECA&D) Report 2008, Publication 224, KNMI, 2008.
- [7] V. Kossobokov, J.-L. Le Mouél and V. Courtillot, "Interactive Comment on 'On Misleading Solar-Climate Relationship' by B. Legras, *et al.*," *Climate of the Past Discussions*, Vol. 6, 2010, p. C342. <http://www.clim-past-discuss.net/6/C342/2010/cpd-6-C342-2010.pdf>
- [8] R. R. McKittrick and P. J. Michaels, "Quantifying the Influence of Anthropogenic Surface Processes and Inhomogeneities on Gridded Global Climate Data," *Journal of Geophysical Research*, Vol. 112, 2007, Article ID: D24S09. [doi:10.1029/2007JD008465](https://doi.org/10.1029/2007JD008465)
- [9] J.-L. Le Mouél, E. Blanter, M. Shnirman and V. Courtillot, "Evidence for Solar Forcing in Variability of Temperatures and Pressures in Europe," *Journal of Atmospheric and Solar-Terrestrial Physics*, Vol. 71, 2009, pp. 1309-1321. [doi:10.1016/j.jastp.2009.05.006](https://doi.org/10.1016/j.jastp.2009.05.006)
- [10] M. Kottek, J. Grieser, C. Beck, B. Rudolf and F. Rubel, "World Map of the Köppen-Geiger Climate Classification Updated," *Meteorologische Zeitschrift*, Vol. 15, No. 3, 2006, pp. 259-263. [doi:10.1127/0941-2948/2006/0130](https://doi.org/10.1127/0941-2948/2006/0130)